Photoacoustic Detection of Protein Coagulation in Albumen-Based Phantoms

Robin F. Castelino*[a, b], William M. Whelan[c, d], Michael C. Kolios[a, b, d]
[a]Department of Electrical and Computer Engineering, Ryerson University, Toronto, Canada
[b]Department of Medical Biophysics, University of Toronto, Toronto, Canada
[c]Department of Physics, University of PEI, Charlottetown, Canada
[d]Department of Physics, Ryerson University, Toronto, Canada

ABSTRACT

Photoacoustic tomography provides good optical contrast with high spatial resolution making it an attractive tool for noninvasive imaging. While the mechanical parameters of tissue affect the photoacoustic signal, the differences in optical absorption mainly determines the contrast between different media. In this work we investigate how the variation in optical and mechanical properties during laser-induced coagulation can be detected by changes in the amplitude and temporal characteristics of photoacoustic signals. Photoacoustic pressure profiles are investigated for tissue equivalent albumen phantoms exposed to varying thermal doses, simulating thermal coagulation. Illumination is performed using an optical parametric oscillator (OPO) fed by a Q-switched Nd:YAG pulsed laser to illuminate at multiple wavelengths. The results of the study demonstrate that photoacoustic signals are sensitive to changes in delivered thermal dose and, hence, photoacoustic imaging has potential as a non-invasive monitoring tool for thermal therapy.

Keywords: photoacoustic imaging, photoacoustic monitoring, thermal therapy, albumen phantom, thermal dose

1. INTRODUCTION

Photoacoustic tomography (PAT) also called optoacoustic or thermoacoustic tomography in biological tissues can be described as optically induced ultrasound imaging; however it is significantly different from traditional ultrasound imaging.[1, 2] In PAT, the acoustic waves are created within the tissue and primarily depend on the contrast between the optical and mechanical properties of the absorber and the surrounding media, thus enhancing the differences of the targeted tissue and surrounding. Laser pulses directed at targeted tissue, at most, raise the temperature by a fraction of a degree; and like ultrasound, PAT has the benefit over positron emission tomography, computer tomography and x-ray imaging methods in that ionizing radiation is not used.

PAT has the benefits of optical and ultrasound imaging systems – good optical contrast and high spatial resolution. It inherently overcomes the problems of loss in resolution and sensitivity due to light scattering in pure optical imaging as well as poor tissue contrast associated with conventional ultrasound imaging.[1, 3, 4]

Minimally invasive thermal therapy (TT) has been explored as a means of treating small solid tumours with minimal damage to adjacent soft tissue by achieving coagulative necrosis in a targeted tumour region over a period of a few minutes. Coagulation occurs between 55°C and 95°C and can be characterized by a change in the tissue optical and mechanical properties.[5] Laser TT was introduced by Bown and has been investigated by researchers as an alternative treatment modality for many tumours including the breast, liver and prostate.[6-9]

A major challenge in the delivery of thermal therapy (TT) is to provide complete tumour coverage without thermally damaging the surrounding healthy tissue. Due to the dynamic changes in temperature, and optical and mechanical properties during TT, accurate pre-treatment planning models are difficult to achieve. Since there is a large variability in the type of response between patients and tissues, a solution to minimize risk and account for dynamic changes is needed

*corresponding author: robin.castelino@sri.utoronto.ca

Photons Plus Ultrasound: Imaging and Sensing 2008: The Ninth Conference on Biomedical Thermoacoustics, Optoacoustics, and Acousto-optics, edited by Alexander A. Oraevsky, Lihong V. Wang, Proc. of SPIE Vol. 6856, 685626, (2008) · 1605-7422/08/$18 · doi: 10.1117/12.764305

such as a feedback monitoring and control system. Various minimally or non-invasive methods of guiding and monitoring TT are being investigated including fluoroptic temperature sensors, magnetic resonance temperature imaging, the use of radiance/fluence probes and ultrasound imaging.[10-13]

There are several benefits in using PAT as a guiding and monitoring system in TT. It has the potential to accurately discriminate a tumour from the surrounding normal tissue and then provide an effective means of real-time mapping of treatment progression since the changes in the tumour optical and mechanical properties can be identified. This will ensure the least amount of damage to surrounding healthy tissue. PAT has an advantage over pure optical and ultrasound techniques due to its hybrid nature, as it is sensitive to both optical and mechanical changes in the tissue.

In this work we investigate how the variation in optical and mechanical properties during laser-induced tissue coagulation can be detected by changes in the amplitude and temporal characteristics of photoacoustic signals using tissue equivalent albumen phantoms.

2. THEORY

Photoacoustic (PA) waves can be described by the change in pressure $\Delta P(z)$:[2, 14]

$$\Delta P(z) = \Gamma \mu_a \Psi(z) \tag{1}$$

where Γ is the Grüneisen parameter, $\Psi(z)$ [J/cm^2] is the laser fluence at depth z and μ_a is the optical absorption coefficient of the target absorber. The Grüneisen parameter, Γ, is a dimensionless quantity which represents thermoacoustic efficiency. It is a temperature dependent factor proportional to the fraction of thermal energy converted into mechanical stress and can be expressed as:[1]

$$\Gamma = \frac{M\beta}{\rho C_P} = \frac{\beta c^2}{C_P} \tag{2}$$

where M [Pa] is the bulk modulus, ρ [g/cm^3] is density, C_p [J/gK] is the heat capacity at constant pressure and β [K^{-1}] is the thermal coefficient of volume expansion of the sample. At 20°C, Γ = 0.1 for water and aqueous solutions. In comparison for fats, lipids, and oils, Γ = 12.7 and as such are efficient biological media for PA generation in the presence of chromophores that would absorb light.[1] Within the range of 4°C to 100°C in liquid water the Grüneisen parameter can be expressed by: [1, 15]

$$\Gamma(T_C) = -0.0000236T_C^2 + 0.007T_C - 0.033 \tag{3}$$

where T_C is measured in degrees Celsius.

For thermal therapy, tissue damage can be quantified in terms of equivalent time exposure at 43°C given by an exponential time-temperature relationship, t_{43}, and is known as thermal dose. It is described by the equivalent time it would take to produce the same biological damage if tissue is exposed at 43°C for any arbitrary time-temperature profile. It can be calculated from the time-temperature history using:[16]

$$t_{43} = \int_{t_{initial}}^{t_{final}} C^{(43-T)} dt \tag{4}$$

where t_{43} is the equivalent time at 43°C and T is the history of the time-temperature between $t_{initial}$ and t_{final} and

$$C = \begin{cases} 0.25 & for\ T < 43^\circ C \\ 0.5 & for\ T \geq 43^\circ C \end{cases} \tag{5}$$

Thermal dose is a measure that, in its strictest sense, is used to quantify damage to living cells when exposed to heat. However, thermal dose calculations based on an Arrhenius damage model (for which Eq. 4 is an approximation) have been used in investigations of albumen-based phantoms.[17]

3. METHODS AND MATERIALS

3.1 Photoacoustic Experimental Setup

Laser light is delivered using a Vibrant B 532 (Opotek Inc., Carlsbad, CA, USA) laser system fed by a Q-switched Nd:YAG laser at 1064nm with a pulse duration of ~6.5ns and a repetition rate of 10Hz. The maximum output power of the Nd:YAG laser is 800mJ/pulse with a beam diameter of ~9mm. This source is input into an optical parametric oscillator (OPO) which provides output wavelengths that are tunable between 680nm – 950nm, delivering a maximum power output of 75mJ/pulse at ~710nm. The output of the OPO is the irradiation source. An optical engineered diffuser (RPC Photonics, Rochester, NY, USA) is used to homogenize and diffuse the beam to provide a uniform fluence field before illuminating the target sample from the top. The pulse energy density on the sample surface is limited to ~5mJ/cm^2 – well below the maximum permissible exposure for human skin as specified by ANSI.

The PA imaging system, as described by *Wang et al.*, has one ultrasonic detection channel which can receive PA signals[18]. A variety of ultrasonic transducers can be used, however, in this work, a transducer having a central frequency of 1MHz (Panametrics–NDT V-303), with an active surface diameter of 10mm, is used. The nominal bandwidth of the transducer is approximately 60% of the central frequency. The transducer converts the laser-induced photoacoustic waves into electrical signals that are amplified by a low noise power amplifier (Panametrics 5670). It is connected to a motor driven rotary table which sequentially moves with a variable step size (typically between 1° – 3°) in a circular manner. An oscilloscope card (National Instruments NI-5112) digitizes the photoacoustic signal. It is controlled by LabView which synchronizes the acquisition from the trigger generated when the laser fires and then automates the data acquisition and positioning of the transducer.[19] Finally, an image is reconstructed using a radial back-projection (RBP) algorithm by mapping the absorption of light using the information contained within the acoustic waves that were detected and stored from all the different transducer locations.[19, 20]

3.2 Tissue Mimicking Albumen Phantom

Albumen-based coagulating phantoms were fabricated based on the procedure described by *Iizuka et al.* [21]. Albumen was chosen because it is homogeneous, uniform in appearance and responds to heat similar to tissue (i.e. coagulates). It is comprised mainly of water (88.1%), globular proteins (10.2%) and lipids (0.05%) and is commercially available in powdered form. Exposure to heat causes the albumen proteins to denature which produces a visible whitening and is characterized by an increase in optical scattering, similar to tissues.[22]

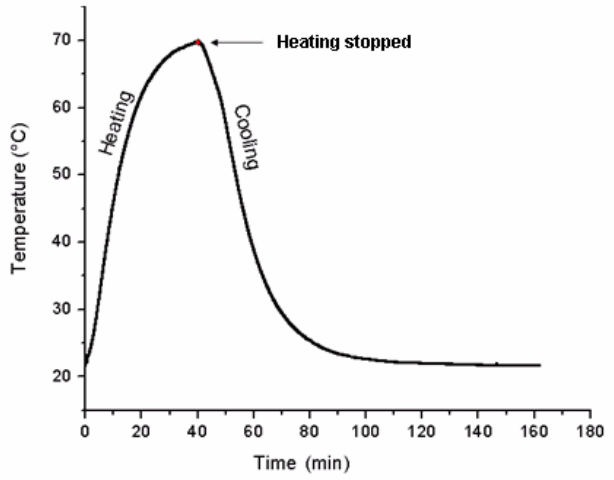

Fig 1. Temperature profile at the centre of an albumen phantom submerged in a 70°C water bath

Nine cylindrical shaped phantoms were made, 5 cm in diameter and 3 cm thick. A thermocouple was inserted at the centre. The phantom was then enclosed in a waterproof container and heated in a water bath at 70°C. When the centre reached 70°C, the phantom was immediately cooled by placing it into another water bath at room temperature. The nine phantoms were heated in five minute heating intervals from zero minutes to forty minutes. A typical heating/cooling profile is shown in Figure 1.

To investigate the influence of coagulation (which is related to thermal dose) on the PA signals, 10mm diameter samples were removed from the centre of each phantom and imaged to minimize the effects of gradient heating (i.e. the edges of the phantoms would have a higher thermal dose than the centre). The signals were produced by illuminating the samples at 740nm. Another experiment using an illumination wavelength of 810nm produced very similar results, therefore only data at 740nm is presented here. Twelve measurements are taken from around the phantom separated by 30° step increments. Each set of twelve measurements has a signal to signal deviation of less than 5%.[19] The twelve signals are averaged to produce one signal per phantom by aligning the data with respect to the positive peak.

4. RESULTS AND DISCUSSION

Using the measured heating/cooling profiles, the delivered thermal dose for all phantoms was calculated according to Equation 4. In addition, the optical properties of each phantom were measured using a double integrating sphere (DIS) system[23]. Thermal dose and optical property values are shown in Table 1.

Table 1. Optical Properties at 740nm and thermal dose values for nine albumen phantoms

Minutes Heated	Max Temp (°C)	Thermal Dose (eq. min)	μ_a [cm^{-1}]	μ_s [cm^{-1}]	μ_{eff} [cm^{-1}]
0	21	0	1.11	10.35	2.67
5	31.7	0.08	1.12	15.17	2.97
10	45.6	547.92	1.20	23.01	3.55
15	55.5	5.49×10^5	1.22	40.44	4.38
20	61.7	5.42×10^7	1.30	67.69	5.60
25	65.4	7.65×10^8	1.36	126.00	7.54
30	67.7	7.00×10^9	1.48	135.29	8.16
35	68.9	2.34×10^{10}	1.58	151.62	8.91
40	69.7	6.16×10^{10}	1.60	170.77	9.46

When heated, the albumen coagulates causing the phantom to appear white as seen in Figure 2. The degree of visual whitening increases with thermal dose. This whitening can be quantified as an increase in optical scattering (see Table 1). The optical scattering coefficient, μ_s, increased by a factor of ~ 17 after 40 minutes of heating. The dominant chromophore in the phantom preparation is Naphtol Green B, as albumen in its native state has very little absorption in the NIR.[21] After 40 minutes of heating, the optical absorption coefficient, μ_a, increased by 44%. Overall, the effective optical attenuation coefficient, μ_{eff}, increased three fold, primarily due to the large increase in scattering.

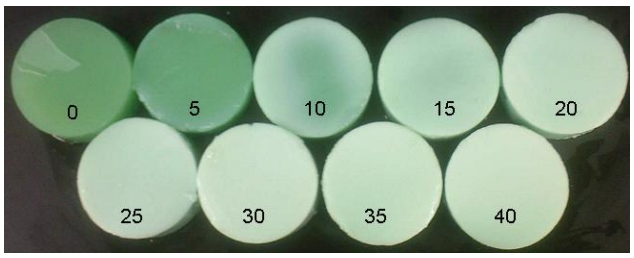

Fig 2. Photograph of albumen phantoms heated for different time periods. The number on each phantom represents the amount of time, in minutes, that each phantom was immersed in the water bath at 70°C

Three independent experiments were conducted for each thermal dose delivered. The average PA signals are presented in Figure 3 with the peaks aligned to improve readability and interpretation.

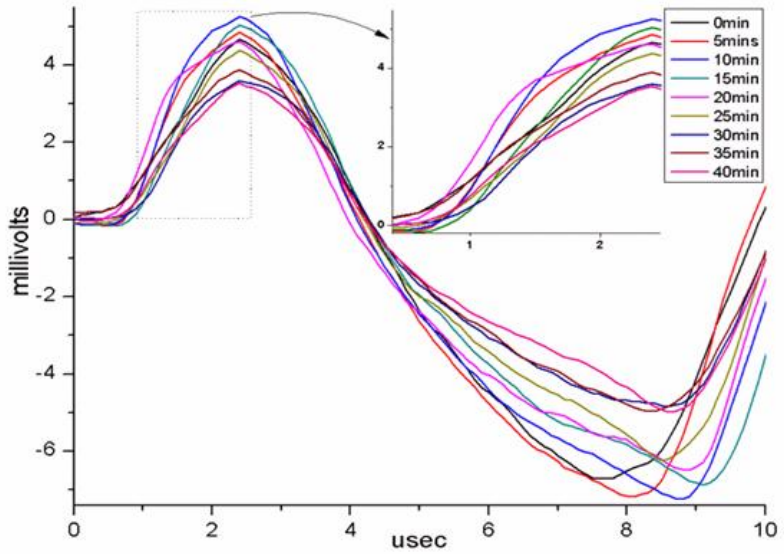

Fig 3. Averaged PA signals measured from tissue mimicking albumen phantoms as a function of heating time.

In examining the detected PA signals in Figure 3, three features were used in the analysis: (i) the positive peak amplitude, (ii) the slope of the rising positive peak and (iii) the peak to peak difference of the PA signal, denoted by A, B and C in Figure 4, respectively.

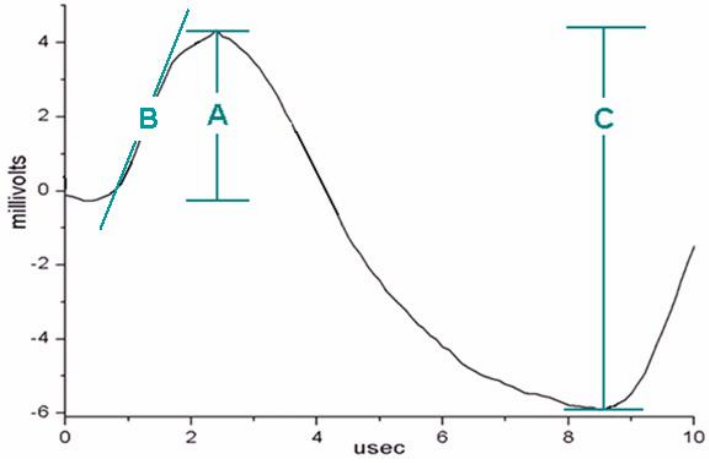

Fig 4. Typical photoacoustic signal denoting features: A - amplitude of the positive peak, B - the slope of the rising positive peak and C - signal peak to peak difference

The differences in these three signal features A, B and C as a function of heating time for each of the three trials are shown in Figure 5 a, b, c, respectively. Two key observations can be made: (i) there are substantial variations in a signal feature between trials and ii) all three signal features, A, B and C increase up to 10 minutes of heating, followed by a decrease as heating continues. Interpreting the heat-induced changes in the signal features is difficult due to the fact that

the generated PA signal is proportional to the product of the optical fluence, the Grüneisen parameter, Γ, and the optical absorption, μ_a (Equation 1). It is assumed that the incident fluence at the surface of the phantom was constant for all experiments. Moreover, the Grüneisen parameter was not measured. However, *Larin et al*, reported that coagulated tissues exhibit an increased Grüneisen parameter which remains even when the tissue cools to room temperature.[15] With the maximum temperature reaching 45.6°C (Table 1) at the centre of the phantom at 10 minutes of heating, it is likely that a very low percentage of albumen was denatured, since the protein denaturation process only commences at around 45°C.[24] However, an 8 % increase in optical absorption was measured during this time (Table 1) which may account for the increase in the peak amplitude (feature A).

The observed decrease in the peak amplitude (feature A) and peak to peak amplitude (feature C) beyond 10 minutes of heating is somewhat surprising given the measured increase in optical absorption (see Equation 1). This suggests that the heat-induced change in optical fluence is playing a dominate role in the generation of PA waves or that there is a change in the Grüneisen parameter. The substantial increase in optical scattering that occurs due to coagulation acts to reduce light penetration into the phantom and alters the energy deposition pattern. Hence, a better understanding of the relationship between spatial energy deposition in a medium and photoacoustic wave generation is needed.

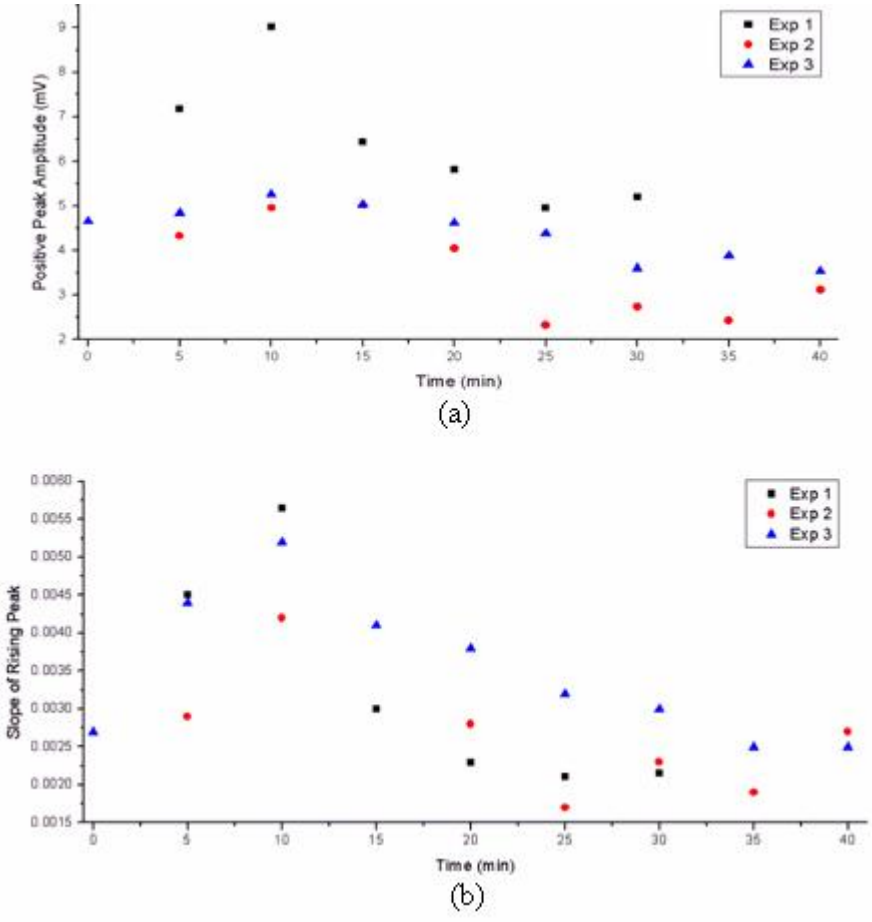

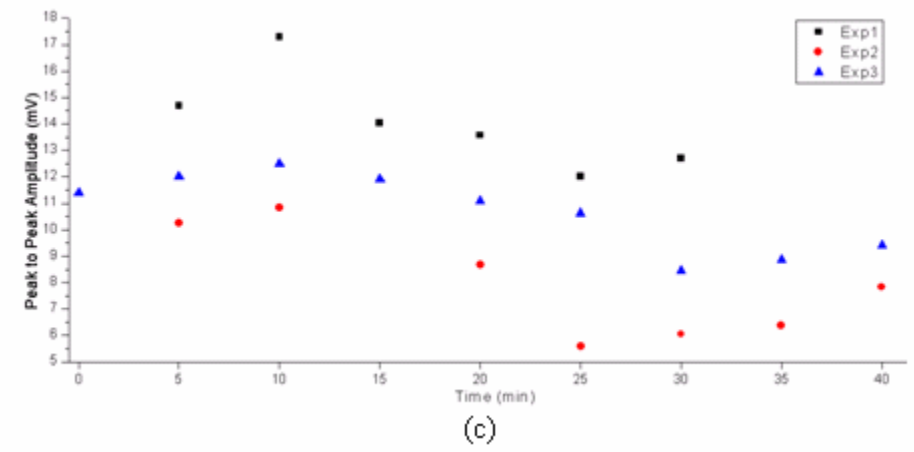

Fig 5. (a) Peak to peak PA signal difference as a function of heating in minutes. (b) Positive PA peak signal amplitude as a function of heating in minutes. (c) PA slope of rising peak as a function of heating in minutes

5. CONCLUSIONS

In this work, three features based on amplitude and temporal characteristics were identified to aid in the analysis of detected photoacoustic signals. Further investigation is needed to better quantify the relationship between these photoacoustic signal features and the changes in optical and mechanical properties of the phantom as a function of thermal dose. The results of the study demonstrate that photoacoustic signals are sensitive to changes in delivered thermal dose in albumen-based coagulating phantoms and therefore, photoacoustic imaging has potential as a non-invasive monitoring tool for thermal therapy.

ACKNOWLEDGEMENTS

The authors would like to gratefully acknowledge Arthur Worthington, Behrouz Soroushian and Barry Vuong for their assistance. Financial support was provided by The Natural Sciences and Engineering Research Council of Canada and the Canadian Institute of Health Research (Collaborative Health Research Project CHRPJ 323745-06) and The Canada Foundation for Innovation (CFI).

REFERENCES

1. Oraevsky, A.A. & Karabuto, A.A. (eds.) Optoacoustic tomography. (CRC, New York; 2003).
2. Gusev, V.E. & Karabutov, A.A. Laser Optoacoustics (AIP, New York; 1993).
3. Ku, G., Wang, X., Xie, X., Stoica, G. & Wang, L.V. Imaging of tumor angiogenesis in rat brains in vivo by photoacoustic tomography. *Applied Optics* **44**, 770-775 (2005).
4. Fan, Y., Mandelis, A., Spirou, G. & Vitkin, I.A. Development of a laser photothermoacoustic frequency-swept system for subsurface imaging: Theory and experiment. *Journal of the Acoustical Society of America* **116**, 3523-3533 (2004).
5. Welch, A.J., Motamedi, M., Rastegar, S., LeCarpentier, G.L. & Jansen, D. Laser thermal ablation. *Photochemistry and Photobiology* **53**, 815-823 (1991).
6. Bown, S.G. Phototherapy of tumors. *World Journal of Surgery* **7**, 700-709 (1983).
7. Hall-Craggs, M.A. & Vaidya, J.S. Minimally invasive therapy for the treatment of breast tumours. *European Journal of Radiology* **42**, 52-57 (2002).
8. Izzo, F. Other thermal ablation techniques: Microwave and interstitial laser ablation of liver tumors. *Annals of Surgical Oncology* **10**, 491-497 (2003).

9. Aho, T.F. & Gilling, P.J. Laser therapy for benign prostatic hyperplasia: A review of recent developments. *Current Opinion in Urology* **13**, 39-44 (2003).
10. Davidson, S.R.H., Vitkin, I.A., Sherar, M.D. & Whelan, W.M. Characterization of measurement artefacts in fluoroptic temperature sensors: Implications for laser thermal therapy at 810 nm. *Lasers in Surgery and Medicine* **36**, 297-306 (2005).
11. Hazle, J.D., Stafford, R.J. & Price, R.E. Magnetic resonance imaging-guided focused ultrasound thermal therapy in experimental animal models: Correlation of ablation volumes with pathology in rabbit muscle and VX2 tumors. *Journal of Magnetic Resonance Imaging* **15**, 185-194 (2002).
12. Chin, L.C.L., Wilson, B.C., Whelan, W.M. & Vitkin, I.A. Radiance-based monitoring of the extent of tissue coagulation during laser interstitial thermal therapy. *Optics Letters* **29**, 959-961 (2004).
13. Veltri, A. et al. Percutaneous US-guided RF thermal ablation for malignant renal tumors: Preliminary results in 13 patients. *European Radiology* **14**, 2303-2310 (2004).
14. Oraevsky, A.A., Jacques, S.L. & Tittel, F.K. Measurement of tissue optical properties by time-resolved detection of laser-induced transient stress. *Applied Optics* **36**, 402-415 (1997).
15. Larin, K.V., Larina, I.V. & Esenaliev, R.O. Monitoring of tissue coagulation during thermotherapy using optoacoustic technique. *Journal of Physics D: Applied Physics* **38**, 2645-2653 (2005).
16. Sapareto, S.A. & Dewey, W.C. Thermal dose determination in cancer therapy. *International Journal of Radiation Oncology Biology Physics* **10**, 787-800 (1984).
17. Iizuka, M.N., Vitkin, I.A., Kolios, M.C. & Sherar, M.D. The effects of dynamic optical properties during interstitial laser photocoagulation. *Physics in Medicine and Biology* **45**, 1335-1357 (2000).
18. Wang, X., Pang, Y., Ku, G., Stoica, G. & Wang, L.V. Three-dimensional laser-induced photoacoustic tomography of mouse brain with the skin and skull intact. *Optics Letters* **28**, 1739-1741 (2003).
19. Castelino, R.F. Biomedical Applications of Photoacoustics for Thermal Therapy. *Master of Applied Science thesis*. (Ryerson University, Toronto, Canada; 2008).
20. Xu, Y., Feng, D. & Wang, L.V. Exact frequency-domain reconstruction for thermoacoustic tomography - I: Planar geometry. *IEEE Transactions on Medical Imaging* **21**, 823-828 (2002).
21. Iizuka, M.N., Sherar, M.D. & Vitkin, I.A. Optical phantom materials for near infrared laser photocoagulation studies. *Lasers in Surgery and Medicine* **25**, 159-169 (1999).
22. Pickering, J.W. Optical property changes as a result of protein denature in albumen and yolk. *Journal of Photochemistry and Photobiology B: Biology* **16**, 101-111 (1992).
23. Prahl, S.A., van Gemert, M.J.C. & Welch, A.J. Determining the optical properties of turbid media by using the adding-doubling method. *Applied Optics* **32**, 559-568 (1993).
24. Bischof, J.C. & He, X. Thermal stability of proteins. *Annals of the New York Academy of Sciences.* **1066**, 12-33 (2005).